

# Operation and Plume Measurements of Miniaturized Cylindrical Hall Thrusters with Permanent Magnets

Yevgeny Raitses,<sup>\*</sup> Enrique Merino,<sup>§</sup> Jeffrey B. Parker,<sup>\*\*</sup> and Nathaniel J. Fisch<sup>§</sup>  
*Princeton Plasma Physics Laboratory, Princeton University, Princeton, NJ, 08543*

Two permanent magnet versions of the miniaturized cylindrical Hall thruster (CHT) with different channel outer diameters, 1.5 cm and 2.6 cm, were operated in the power range of 50W-300 W. With twice smaller total power consumption, the 2.6 cm CHT is twice lighter than its electromagnet counterpart. Results of the discharge and plasma plume measurements suggest that the CHT with permanent magnets and electromagnet coils operate rather differently. In particular, the plasma flow from the permanent magnet thrusters has an unusual halo shape of the angular ion current density distribution with a majority of high energy ions flowing at the angles of 50°-70° with respect to the thruster centerline. This divergence of the energetic ion flow leads to the reduced efficiency of the thrust production in these thrusters.

## I. Introduction

The cylindrical Hall thruster<sup>1</sup> (CHT) features a combination of both end-Hall thruster<sup>2</sup> (EHT) and conventional annular Hall thrusters of stationary plasma thruster<sup>3</sup> (SPT) type. The schematic of the CHT is shown in Fig. 1. Like the EHT, the CHT has a lower surface-to-volume ratio than do SPT and, thus, seems to be more promising for scaling down to low power space applications. The principle of operation of the CHT is in many ways similar to that of a typical annular Hall thruster, i.e., it is based on a closed  $E \times B$  electron drift in a quasineutral plasma. However, the CHT differs fundamentally from a conventional annular thruster in that magnetized electrons in the cylindrical design provide charge neutralization of non-magnetized ions not by not moving axially, but through being trapped axially in a hybrid magneto-electrostatic trap.<sup>4</sup> A similar axial trap for electrons should exist in the mirror-type magnetic configuration of the EHT. However, the electron cross-field transport in the CHT is suppressed much better than in the EHT.<sup>5</sup> As a result, the CHT can operate more efficient at higher discharge voltages ( $> 300$  V) to produce high Isp ( $\geq 1500$  sec).

The magnetic field configuration of the CHT can be cusp-type and magnetic mirror-type.<sup>1</sup> Comprehensive studies of the CHT with electromagnet coils are reported elsewhere.<sup>1,4</sup> For the miniaturized 100-200 W-class CHTs, the optimal magnetic field configuration was shown to be an enhanced mirror-type (the so-called direct configuration).<sup>6</sup> The highest thruster performance parameters were achieved when the maximum magnetic field at the mirror was  $\sim 1$ -1.5 kGauss.<sup>7</sup> In these regimes, the electromagnet coils consumed 50-100 W. For the low power thruster, this additional power consumption reduces drastically the overall thruster efficiency. Therefore, the use of permanent magnets instead of electromagnet coils appears to be a natural choice for the low power CHT. In addition to a significant reduction of the total electric power consumption, the use of permanent magnets makes the thruster much lighter than the thruster with electromagnet coils. In this paper, we describe results of discharge and plume measurements for two miniaturized versions of the CHT with permanent magnets (CHTpm), 1.5 cm (channel diameter) CHTpm and 2.6 cm CHTpm. In addition, the effect of the cathode placement with respect to the thruster axis on the thruster operation and the plasma plume is also presented. These results are compared with the discharge and plume characteristics of the 2.6 cm and 3 cm CHT thrusters with electromagnet coils (CHTem). Both CHTem thrusters were comprehensively characterized in our previous works.<sup>4</sup> A part from these operating and plume characterization experiments, thrust measurements for the 2.6 CHTpm at the NASA Marshall SFC are described in a separate paper.<sup>8</sup> Finally, preliminary results of high speed imaging of the plasma in the CHTpm are presented.

<sup>\*</sup> Research Physicist, PPPL, MS-17, P.O. Box 451, Princeton NJ 08543, AIAA Member.

<sup>§</sup> Research Assistant, MS-16, P.O. Box 451, Princeton NJ 08543.

<sup>\*\*</sup> Graduate Student, MS-16, P.O. Box 451, Princeton NJ 08543

<sup>§</sup> Professor, Princeton University and PPPL, MS-1730, P.O. Box 451, Princeton NJ 08543, AIAA Member.

## II. Permanent magnet CHT thrusters

A typical CHT (Fig. 1) consists of a cylindrical ceramic channel, a ring-shaped anode, which serves also as a gas distributor, a magnetic core, and electromagnet coils or permanent magnets.<sup>1,9</sup> The channel can be with or without a short annular part (Fig. 1a and b, respectively),<sup>10,11</sup> which serves to maintain a high ionization of the propellant gas and a strong magnetic insulation of the anode.<sup>12</sup> Although performances of the CHTs with and without annular part are comparable,<sup>10</sup> the absence of the annular channel part adds more simplicity to the CHT design.

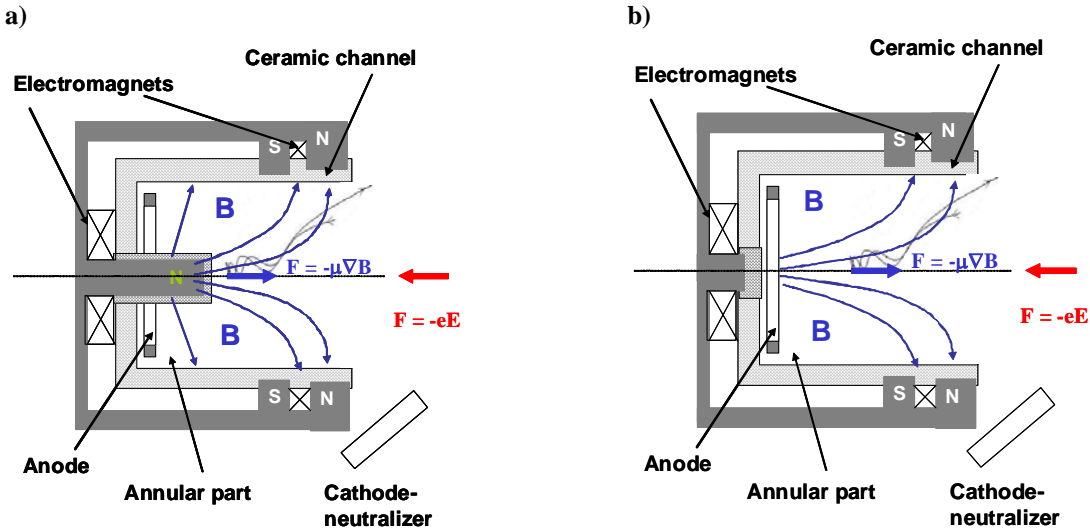


**Figure 1. Schematic of a cylindrical Hall thruster (CHT) with (a) and without (b) a short annular part. The thruster can use electromagnet coils or permanent magnets to form direct (enhanced mirror) or cusp magnetic field configurations.**

In previous studies, we used the 2.6 cm and 3 cm cylindrical thrusters with electromagnet coils.<sup>4,7,9</sup> Fig. 2 shows two laboratory CHTpm thrusters with of the outer diameter of 1.5 cm and 2.6 cm. These thrusters are designed to operate in the input power range of 50-100 and 100-200 W, respectively. The overall dimensions of the CHTpm

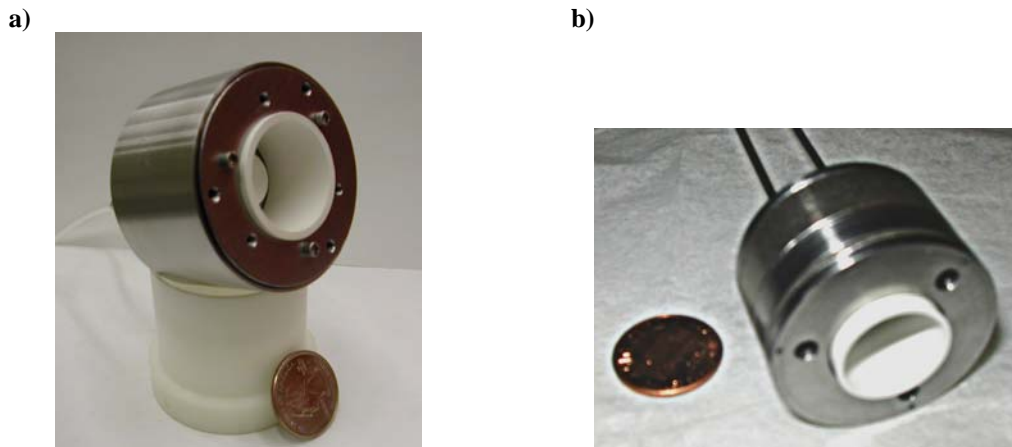


**Figure 2. The laboratory 50-200 W CHT thrusters with Co-Sm permanent magnets (CHTpm): a) 2.6 cm CHTpm with the overall dimensions of 5.5 cm Diameter × 3.5 cm Length (thruster mass is 350 g) and b) the 1.5 cm CHTpm with the overall dimensions of of 3.4 cm Diameter × 2.4 cm Length (110 g).**

thrusters are as follow: for the 2.6 cm CHTpm, 5.5 cm Diameter  $\times$  3.5 cm Length; for the 1.5 cm CHTpm, 3.4 cm Diameter  $\times$  2.4 cm Length. For comparison, the 2.6 CHTem is 7.8 cm Diameter  $\times$  7 cm Length. In addition, the 2.6 CHT pm is twice lighter (350 g) than its counterpart with electromagnetic coils. The thruster mass of the smaller 1.5 cm CHTpm is 110 g. In the described experiments, the 2.6 cm CHTpm had a purely cylindrical channel configuration, while the cylindrical channel of the 1.5 cm CHTpm had a short ( $<2$  mm) annular part.

Each CHTpm thruster uses two permanent magnet rings made from a cobalt-samarium alloy. Like in the thruster with electromagnet coils, these magnet rings are incorporated into the magnetic circuit. Figs. 3 and 4 show results of simulations of the magnetic field produced in the CHTpm thrusters. In order to implement the direct (enhanced mirror) configuration of the CHT both permanent magnet rings have the same polarity (Fig. 3a). For the cusp configuration (Fig. 3b), these rings have an opposite polarity.

Note that a similarity between the magnetic field distributions produced with electromagnets and permanent magnets exists only inside the thruster channel. In the region outside the channel, the permanent magnet rings produce a much stronger magnetic field than in the CHTem case. Moreover, unlike the direct CHTem, the CHTpm has still a cusped magnetic field near the channel exit (Fig. 3b).

### III. Experimental setup

The thrusters were operated in the large PPPL Hall Thruster facility.<sup>13</sup> The xenon gas was used in all experiments. The background pressure in a 28 m<sup>3</sup> vacuum vessel equipped with cryopumps did not exceed 3  $\mu$ torr.

A commercial Heatwave 250 model hollow cathode electron source is used as the cathode-neutralizer. The cathode was placed on a motorized X-Y table in order to change its placement with respect to the thruster axis. The magnetic field in the area of the cathode placement variations is shown in Fig. 4. In these experiments, the cathode gas (Xenon) flow rate was maintained constant, 2 sccm. The cathode keeper electrode was used to initiate the main discharge between the cathode and the thruster anode, and to maintain the discharge current. The keeper current was 0.5 A during the thruster operation.

The plasma plume diagnostics used in these experiments included a planar plume probe with guarding ring for measurements of the angular ion flux distribution in the plume,<sup>13</sup> a bi-directional probe for measurements of the direct ion flux from the thruster and the back ion flux from the background plasma<sup>14</sup> and a two-grid retarding potential analyzer (RPA) for

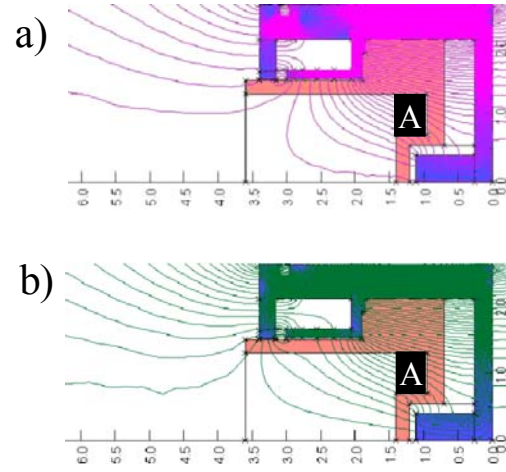


**Figure 3. Magnetic field (simulations) in the 2.6 cm diameter CHT with permanent magnets and without a short annular part of the channel for the cusp (a) and direct (b) magnetic field configurations. The magnetic field measured at the back wall on the centerline is  $\sim 0.8$ -1 kGauss.**

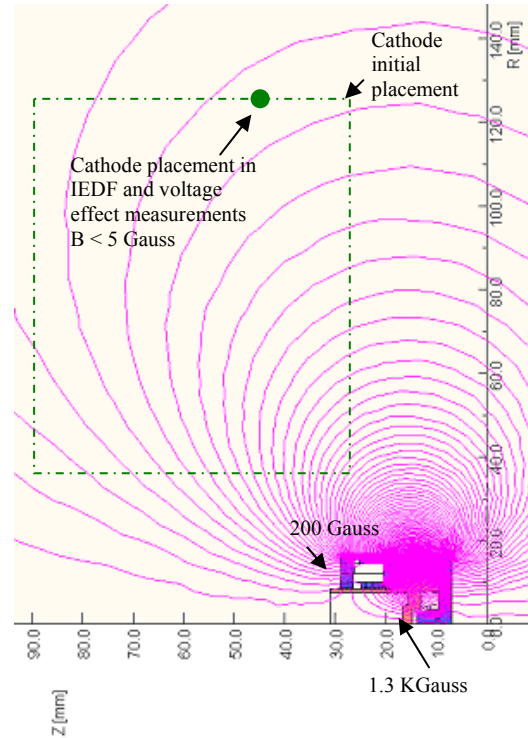


**Figure 4. Magnetic field (simulations) for the 1.5 cm CHTpm of the direct configurations and the area of cathode placements (dashed line) tested in these experiments. Measured magnitudes of the axial component of the magnetic field are indicated for key locations. The dot indicates the cathode placement used in plume measurements at different discharge voltages and the RPA measurements.**

measurements of ion energy distribution function (IEDF). All diagnostic tools are suspended on titanium arms of the rotating platform. The distance between the thruster and rotating plume diagnostics was 73 cm through almost all experiments described in this paper. The exception was IEDF measurements, in which the distance between the thruster and the RPA was about 37 cm.

The measured ion current to the plume probe was corrected to account for background plasma effects.<sup>14</sup> In particular, for each angular position, the measured back ion flux was subtracted from the ion current measured with the guarding ring probe facing the thruster. The total ion current was then estimated by integrating over measured angular ion flux distribution. The propellant and current utilization efficiencies were estimated as the ratios of the corrected ion flux to the mass flow (in unit of current) and the discharge current, respectively. The plume angle was estimated from the measured angular ion flux distribution for 90% of the total ion current.

Finally, for high speed imaging of the thruster plasma, the Phantom V7.3 High Speed Camera was used, and placed about 7 meters from the thruster, looking straight at the thruster channel. Unfiltered emissions in the visible spectrum were recorded

#### IV. Experimental results and discussions

The discharge and plume characteristics of the cylindrical thrusters with permanent magnets are notably different from the corresponding characteristics of typical CHTs with electromagnet coils.<sup>19</sup> For the same discharge voltage and flow rates, the discharge current in the CHTpm is generally smaller than in the CHTem (Fig. 5). The increase of the discharge current with the discharge voltage is mainly associated with the increase of the ion current (Fig. 6). For a typical CHTem, the propellant utilization is unusually high at the discharge voltages of above 200 V. This result was explained by the presence of multi-charged ions, which were measured in the plume of the miniaturized CHT.<sup>11</sup> For the thrusters with permanent magnets, the propellant utilization exceeds 100% at the discharge voltage of above 300-350 V. Moreover, the current utilization efficiency remains relatively low with the increase of the discharge that indicates on the enhancement of the electron cross field current in the CHTpm.

Perhaps the most curious difference between the CHTpm and the CHTem is in the shape of their plumes (Fig. 7).

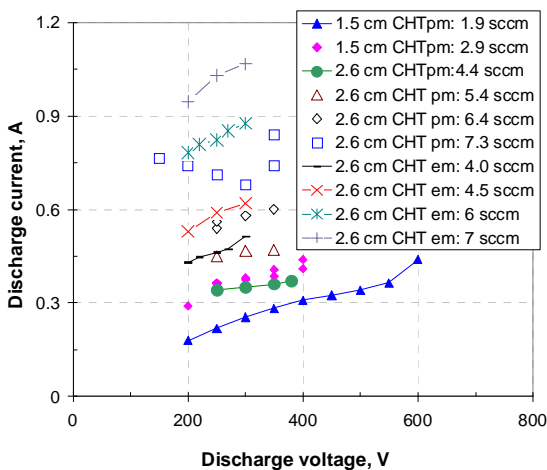


**Figure 5. V-I characteristics of the CHTpm and the CHTem at different flow rates. The magnetic field is constant. For the 2.6 cm CHTs, the cathode placement was near the channel exit.<sup>4</sup> For the 1.5 cm CHTpm, the cathode was at the position shown in Fig. 4.**

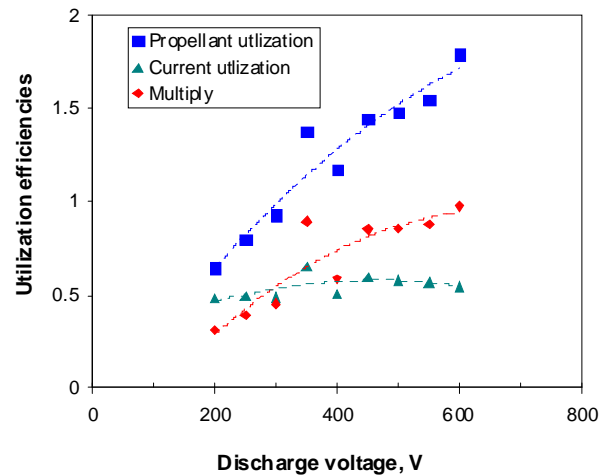


**Figure 6. Utilization efficiencies (propellant, current and propellant times current utilizations). CHT operating parameters: 250 V, 2 sccm of xenon flow. The cathode placement in these measurements is shown in Fig. 4.**

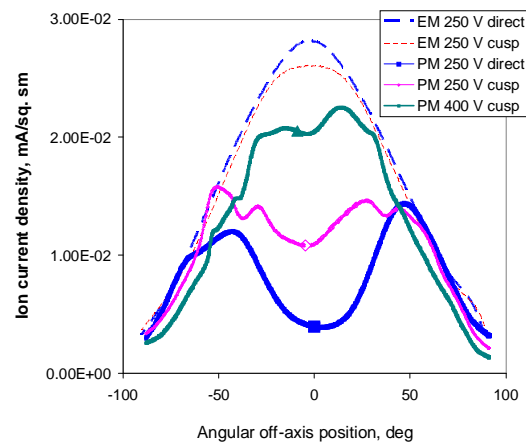


**Figure 7. A comparison of angular ion current distributions measured for the 2.6 cm CHT thruster with electromagnetic coils (EM) at xenon gas flow rate of 3.4 sccm and permanent magnets (PM) at xenon gas flow rate of 4 sccm. The cathode placement was at the channel exit.<sup>4</sup>**

In particular, for the direct configurations, the CHTpm thrusters produce a halo plume with larger ion flux at  $\sim 60^\circ$  with respect to the axis than at the centerline. This shape is changed, but still exists at different cathode placements (Fig. 8). However, the central part of the plume shape undergoes more substantial transformation under variations of the discharge voltage (Fig. 9).

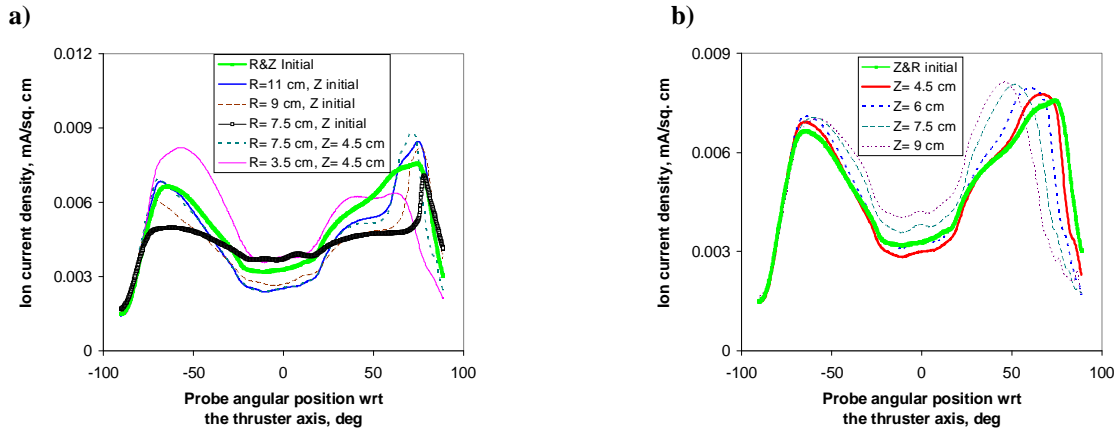


**Figure 8. The effect of the cathode placement with respect to the thruster axis on the plume of the 1.5 cm CHTpm thruster (250 V, 3 sccm of xenon gas flow): varying the cathode placement in a) radial direction and b) axial direction. R and Z coordinates of the cathode placements are shown in Fig. 4.**

Note that the cathode placement was changed in the axial and radial directions (Fig. 8) in the area shown in Fig. 4. The cathode was not brought closer to the thruster axis to avoid its damage in the plume by energetic ions from the thruster. The halo plume shape was also observed when the plume probe was rotating at the shorter distance of 15 cm from the thruster (results of these measurements are not presented in this paper).

Interesting, a similar halo shape of the plume was also observed for different versions of the cylindrical geometry thrusters with cusp and mirror magnetic field, including the MIT diverge-cusped magnetic field thruster (DCF)<sup>15</sup> and, likely, the HEMP thruster<sup>16</sup> (from available plume images and its design similarity with the DCF). However, in the cusp configuration of the CHTpm, the halo shape of the plume is less pronounced (Fig. 7). Furthermore, as the discharge voltage increases, the plume in the vicinity of the centerline seems to be filled out with ion flux. A qualitatively similar effect of the discharge voltage on the plume was also observed for the direct CHTpm (Fig. 9). Here, at high discharge voltages, the plume acquires another unusual shape with multiple peaks of the ion current density.

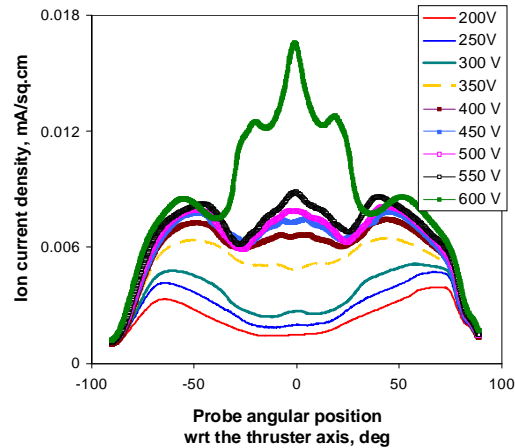


**Figure 9. The effects of the discharge voltage on the plume of the 1.5 cm CHTpm thruster. Thruster operating parameters: 250 V, 2 sccm of xenon flow. The cathode placement in these measurements is shown in Fig. 4.**

Unlike the ion flow in the CHTem and conventional annular Hall thrusters,<sup>17</sup> in the CHTpm, a majority of energetic ions, which contribute to the thrust production, flow at larger angles with respect to the thruster axis ( $50-70^\circ$ ) (Fig. 10). Even at high discharge voltages, when the plume has not a halo shape, the fraction of energetic ions directed along the centerline is apparently smaller than at larger angles (Fig. 11).

We shall briefly discuss the above results of the plume measurements. For all cathode placements used in these experiments (Fig. 4), the magnetic field lines intersecting the cathode intersect also the wall of the cylindrical channel. In addition, the magnetic field between the cathode and thruster is relatively strong (100-200 Gauss) (Fig. 4). Because the electron flow from the cathode to the anode is impeded by this magnetic field outside the thruster, it

is possibly that a strong radial electric field is established in this region. The ions produced and pre-accelerated inside the thruster channel should be deflected by this radial electric field away from the thruster centerline. For example, at low discharge voltages of below 300 V, there are well defined peaks of high energy ions at the centerline and 90° to the thruster centerline. This may be an indication that the acceleration occurs mostly outside the channel. In addition, spatial variations of the ion production inside and outside the channel could also affect the ion trajectories. A combined effect of these variations and ion acceleration inside and outside the channel, as well as their dependence on the discharge voltage should affect the angular distribution of the ion flow, including its shape and the IEDF.

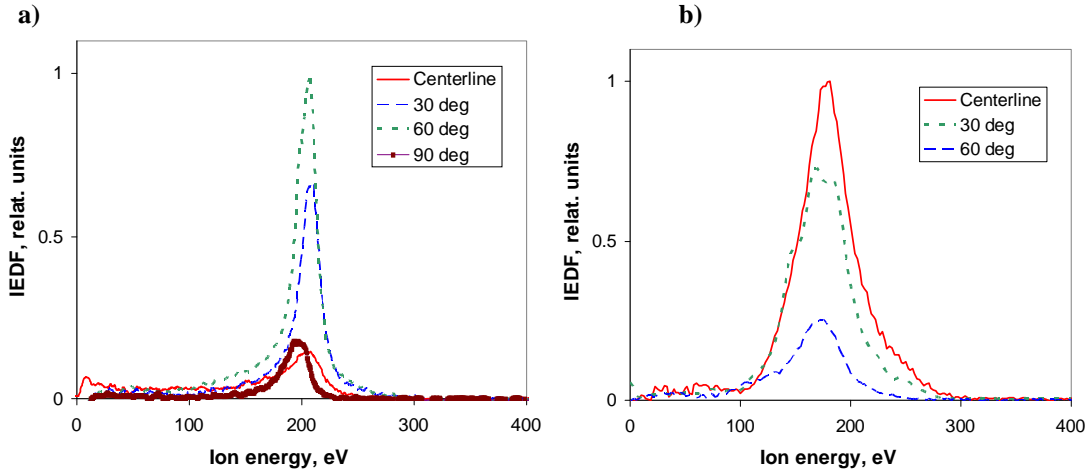


Figure 10. A comparison of the ion energy distribution functions for the CHTs with permanent magnets and electromagnet coils: a) the 1.5 cm CHTpm at xenon gas flow rate of 2 sccm and b) the 3 cm CHTem at xenon gas flow rate of 4 sccm. RPA was at the distance of 37 cm from the 1.5 CHTpm and 73 cm from the 2.6 cm CHTem. For the 1.5 cm CHTpm, the cathode placement is shown in Fig. 4. For the 3 cm CHT, the cathode was placed near the channel exit.<sup>4</sup>

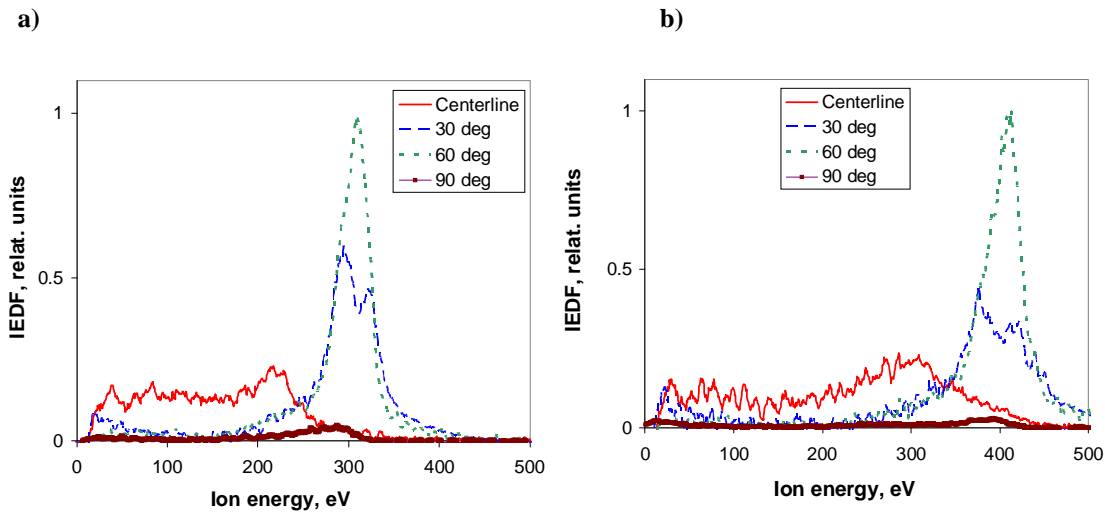
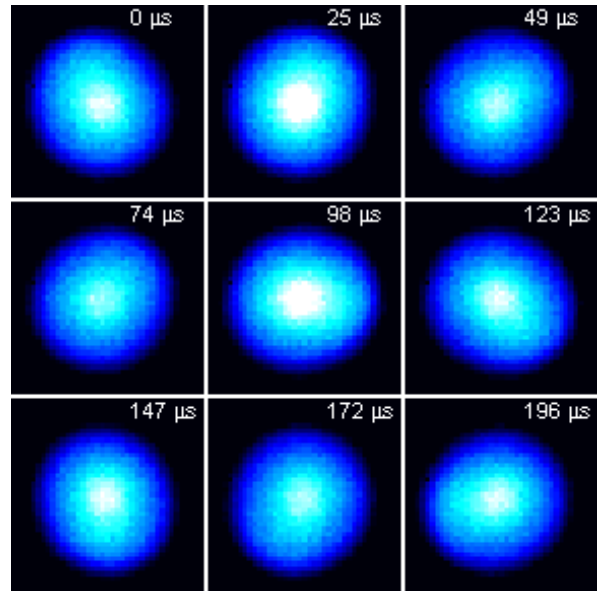


Figure 11. The ion energy distribution function (IEDF) for the 1.5 cm CHTpm at the discharge voltage of a) 350 V and b) 450 V. The IEDFs were obtained from RPA measurements at the distance of 37 cm from the thruster. The xenon gas flow rate was 2 sccm. The cathode placement is shown in Fig. 4.

In addition, dynamic processes in the thruster discharge might also contribute to the formation of the angular distribution of the ion flow and the IEDF. It is known for example, for plasma processing plasmas, that the shape of IEDF at the wall can be affected by an rf-oscillating sheath, when  $\tau_{osc} = 1/f \gg \tau_{tran}$  where  $f$  is the frequency of oscillations and  $\tau_{tran}$  is the transient time, which an ion takes to pass the sheath.<sup>18</sup> For the SPT, the presence of ion-transient oscillations was predicted to broaden the IEDF.<sup>17</sup> In the CHT thrusters, we observed so far two essential modes of oscillations, including the breathing mode,<sup>19</sup> which is usually associated with ionization mechanisms, and a rotational mode. Illustrative images taken with a high speed CCD camera are shown in Fig. 12. Analysis of these images revealed a low frequency rotational oscillation. A “spoke” of light near the outer radius moves azimuthally in the  $\mathbf{E} \times \mathbf{B}$  direction (clockwise above) with a frequency of approximately 3.3 kHz. The breathing oscillations are also visible on these images due to a periodic brightening and dimming of emission. The frequency of the breathing oscillation is about 14 kHz. The breathing oscillations were also detected by measuring time-varying values of the discharge current. Characteristics times of both rotational and breathing modes are longer than a typical ion transient time  $\sim 10^{-5}$ - $10^{-6}$  sec that may be a sufficient condition to alter the angular distribution of the ion flow and the IEDF.



**Figure 12. High speed imaging for the 2.6 CHTpm thruster at the discharge voltage of 250 V. The spoke of light moves azimuthally in the  $\mathbf{E} \times \mathbf{B}$  direction (clockwise) with a frequency of  $\sim 3.3$  kHz.**

#### IV. Concluding remarks

Results of plume measurements for different miniaturized cylindrical Hall thrusters with different magnetizing sources suggest that the operation of the CHTs with permanent magnets is different from the CHTs with electromagnet coils. The ion current density distribution in the plume of the CHTpm has an unusual halo shape with a majority of energetic ions flowing at large angles of  $50^\circ$ - $70^\circ$  with respect to the thruster axis. Apparently, in the CHTpm, the electric field accelerates high energy ions away from the centerline. This is different from the CHTem thrusters, in which high energy ions are accelerated towards the thruster centerline, especially in the current overrun regime<sup>20</sup> (this regime was not achieved with the CHTpm). It is hypothesized that this difference in the ion acceleration between the CHTpm and the CHTem, is because of a relatively strong axial magnetic field outside the channel of the thrusters with permanent magnets. This magnetic field might alter the plasma potential distribution in a way that a significant portion of the ion acceleration occurs outside the channel by a defocusing electric field in this region. Future studies are required to precisely indentify possible steady-state and transient mechanisms which could be responsible for the angular distributions of the ion flow and the IEDF in the CHTpm thrusters.

Finally, curious similarities between the magnetic field outside the channel and the plume shape measured in three permanent magnet versions of the cylindrical thruster, including the CHTpm, DCF and HEMP, suggest that at least with permanent magnets, all three thruster types operate possibly in a similar way. However, the ion flow in the DCF is more focused (the ion current density peaks at  $30^\circ$ - $40^\circ$ ) than in the CHTpm.<sup>15</sup> This result might explain a twice higher anode efficiency of the DCF with permanent magnets ( $\sim 40\%$ ) as compared to the permanent magnet CHT (in Ref. 8). Unlike a traditional CHT design, the DCF and HEMP thrusters employ several cusps distributed along their channels. In view of this design difference, it is interesting to explore the feasibility of optimization of a simpler thruster configuration with a single cusp (like CHT) to narrow the angular distribution of the ion flow.

#### Acknowledgments

The authors wish to thank Prof. Michael Keidar of the George Washington University and Dr. Kurt Polzin of NASA Marshall SFC for fruitful discussion. The authors are also grateful to Dr. Stewart Zweben of the PPPL for his help with high speed imaging of the thruster plasma. This work was supported by the AFOSR.

## References

- <sup>1</sup> Raitsev, Y., and Fisch, N.J., "Parametric Investigations of a Nonconventional Hall Thruster," *Phys. Plasmas*, Vol. 8, No. 5, May 2001, pp. 2579-2586.
- <sup>2</sup> Kaufman, H. R., Robinson, R. S., and Seddon, R. I., "End-Hall ion source", *J. Vac. Sci. Technol. A* 5, 2081 (1987).
- <sup>3</sup> Morozov, A. I., and Savel'ev, V. V., in *Reviews of Plasma Physics*, edited by Kadomtsev, B. B., and Shafranov, V. D., ( Consultants Bureau, New York, 2000), Vol. 21, p. 206.
- <sup>4</sup> Smirnov, A., Raitsev, Y., and Fisch, N. J., "Experimental and theoretical studies of cylindrical Hall thrusters", *Phys. Plasmas* 14, 057106 (2007).
- <sup>5</sup> Raitsev, Y., Smirnov, A., and Fisch, N. J., "Comment on "Effects of magnetic field gradient on ion beam current in cylindrical Hall ion source", submitted to *J. Appl. Phys.*, 2008.
- <sup>6</sup> Smirnov, A., Raitsev, Y., and Fisch, N. J., "Electron cross-field transport in a miniaturized cylindrical Hall thruster", *IEEE Trans. on Plasma Science*, 34, Issue 2, Part 1, pp. 132 – 141, 2006.
- <sup>7</sup> Smirnov, A., Raitsev, Y., and Fisch, N. J., "Electron Cross-Field Transport in a Low Power Cylindrical Hall Thruster", *Phys. Plasmas*, Vol. 11, No. 11, pp. 4922-4933, 2004.
- <sup>8</sup> Polzin, K. A., Sooby, E.S., Kimberlin, A.C., Raitsev, Y., Merino, E., and Fisch, N.J., "Performance of a Permanent-Magnet Cylindrical Hall-Effect Thruster" 45th AIAA/ASME/SAE/ASEE Joint Propulsion Conference, Denver, CO, Aug. 3–5, 2009, AIAA-2009-4812.
- <sup>9</sup> Smirnov, A., Raitsev, Y., and Fisch, N.J., "Parametric investigation of miniaturized cylindrical and annular Hall thrusters", *J. Appl. Phys.* **92**, 5673 (2002).
- <sup>10</sup> Raitsev, Y. and Fisch, N.J., "Cylindrical Geometry Hall Thruster," US Patent No.: 6,448,721 B2, September 2002; Raitsev, Y., Fisch, N.J., Ertmer, K.M., and Burlingame, C.A., "A Study of Cylindrical Hall Thruster for Low Power Space Applications," AIAA 2000-3421, 36th Joint Propulsion Conference, Huntsville, AL, July 2000.
- <sup>11</sup> Diamant, K. D., Pollard, J. E. , Raitsev, Y., and Fisch, N. J., Low power cylindrical Hall thruster performance and plume properties. Presented at the 44th AIAA/ASME/SAE/ASEE Joint Propulsion Conference, Hartford, CT, July 21-23, 2008, AIAA-2008-4998.
- <sup>12</sup> Shirasaki, A. and Tahara, H., "Operational Characteristics and Plasma Measurements in Cylindrical Hall Thrusters," *Journal of Applied Physics* 101, 073307 (2007).
- <sup>13</sup> Raitsev, Y., Staack, D., Dunaevsky, A., Dorf, L., and Fisch, N. J., "Measurements of Plasma Flow in a 2 kW Segmented Electrode Hall Thruster", in the proceedings of the 28th International Electric Propulsion Conference, Toulouse, France, March 2003, IEPC paper 03-0139
- <sup>14</sup> Raitsev, Y., Moeller, T., Szabo, J., "AEDC plume measurements using bi-directional ion flux probes", in the proceedings of the 30<sup>th</sup> International Electric Propulsion Conference , Florence, Italy, September 17-20, 2007, IEPC paper 2007-334.
- <sup>15</sup> Courtney, D. G., Lozanoy, P., and Martinez-Sanchez, M., "Continued Investigation of Diverging Cusped Field Thruster", 44th AIAA/ASME/SAE/ASEE Joint Propulsion Conference & Exhibit, 21 - 23 July 2008, Hartford, CT, AIAA paper 2008-4631.
- <sup>16</sup> Koch, N., Harmann, H.-P., Kornfeld, G." Development and test status of the THALES high efficiency multistage plasma (HEMP) thruster family" IEPC paper 2005-297 Proceedings of the 29th International Electric Propulsion Conference, Princeton, NJ, Oct. 2005.
- <sup>17</sup> Bareilles, J., Hagelaar, G. J. M., Garrigues, L., Boniface, C., Boeuf, J. P., and Gascon, N., "Critical assessment of a two-dimensional hybrid Hall thruster model: Comparisons with experiments ", *Phys. Plasmas* 11 3035 (2004)
- <sup>18</sup> Kawamura, E., Vahedi, V., Lieberman, M. A., and Birdsall C. K., "Ion energy distributions in rf sheaths; review, analysis and simulation", *Plasma Sources Sci. Technol.* 8 No 3 (August 1999) R45-R64
- <sup>19</sup> "Effects of enhanced cathode electron emission on Hall thruster operation", *Phys. Plasmas* 16 057106 (2009).
- <sup>20</sup> Raitsev, Y., Smirnov, A., and Fisch, N. J., "Enhanced performance of cylindrical Hall thrusters", *Appl. Phys. Lett.* 90, 221502 (2007).